Numerical Simulations of the Flooding inside a Damaged Cabin with Horizontal and Vertical Baffles by MPS Method

MARINE 2023

Congyi Huang, Weiwen Zhao, Decheng Wan*

Computational Marine Hydrodynamic Lab (CMHL), School of Naval Architecture, Ocean and Civil Engineering, Shanghai Jiao Tong University, Shanghai, China

*Corresponding Author: dcwan@sjtu.edu.cn

ABSTRACT

In recent years, shipwrecking accidents occur frequently, which may bring danger to structures and people aboard. Therefore, it is of great significance to simulate the flooding process inside a damaged cabin and predict rescue time. In this paper, the flooding inside a two-dimensional cabin is simulated by the inner solver MPSGPU-SJTU, which is based on the MPS algorithm and GPU platform. Firstly, the accuracy and stability of the solver are verified by simulating the water intake process of a damage cabin. The simulated horizontal and vertical displacements of the cabin are in good agreement with the published results. Then, the flooding process inside the damaged cabin with horizontal and vertical baffles is simulated. The influence of the position of the baffle on reducing the horizontal and vertical displacement as well as the roll angle of the damaged cabin is analyzed.

Keywords: MPS method; MPSGPU-SJTU solver; damaged tank; flooding.

1. INTRODUCTION

With the rapid development of sea transportation, maritime accidents occur frequently. The broken cabin will be flooded, resulting in instability of the ship, which will make the people on board in danger. Therefore, it is very important to study the inflow process and the dynamic behavior of the damaged hull. As a meshless method, MPS has the Lagrangian property of tracking the motion of particles and can accurately capture the free surface. Therefore, it is widely used to deal with the problems with large deformation of free surface in recent years. Many researches on the damaged cabin have been carried out based on the meshless method. Cao et al. (2018) simulated the blooding process of the broken hull by a multiphase SPH model. The effect of air was also taken into account. Gonz ález et al. (2003) used SPH method to predict the dynamic response of damaged RO-RO ships and the green water process. Touz é et al. (2010) used SPH method to predict the water inflow at the moment of collision between two ships in waves. Shen & Vassalos (2009) simulated the blooding process of a damaged cabin under rolling and heave motion based on SPH method. Zhang et al. (2013) applied the three-dimensional SPH method to simulate the blooding and sinking process of the ship model damaged on the side. Ming et al. (2018) conducted a study on the blooding process of a damaged cabin in transverse regular waves based on the weakly compressible smooth particle hydrodynamics (WCSPH) method. Zhang et al. (2020) simulated the water blooding process of two-dimensional broken cabin and analyzed the influence of opening and baffle position on the water inflow.

2. NUMERICAL METHOD

The MPS method is a meshless particle method based on the Lagrange representation. The computational domain is represented by discrete particles. These particles are not connected by grids or nodes, but carry physical quantities such as mass, velocity and acceleration separately. The flow field is controlled by establishing the governing equation.

2.1 Governing equations

The governing equations include the continuity equation and the momentum equation. The governing equation for viscous incompressible fluid can be written as:

$$\frac{1}{\rho}\frac{D\rho}{Dt} = -\nabla \cdot \boldsymbol{V} = 0 \tag{1}$$

$$\frac{D\boldsymbol{V}}{Dt} = -\frac{1}{\rho}\nabla P + \nu \nabla^2 \boldsymbol{V} + \boldsymbol{g} \tag{2}$$

where ρ is fluid density, $\boldsymbol{V}$ is velocity vector, P presents pressure, ν is kinematic viscosity, $\boldsymbol{g}$ is gravitational acceleration vector, t indicates time.

2.2 Discretization of the governing equations

In the MPS method, the computational domain is composed of discrete particles. Therefore, the governing equations need to be discretized.

2.2.1 Kernel function

In the MPS method, the interaction between particles is realized by the kernel function, which can be written as:

$$W(r) = \begin{cases} \dfrac{r_e}{0.85r + 0.15r_e} - 1 & 0 \le r < r_e \\ 0 & r_e \le r \end{cases} \tag{3}$$

where $r = |\boldsymbol{r}_j - \boldsymbol{r}_i|$ represents the distance between particle i and j, r_e is the influence radius.

2.2.2 Density of the particle number

The particle number density is the sum of kernel functions of all the particles within the influence radius, which can be written as:

$$\langle n \rangle_i = \sum_{j \ne i} W\left(|\boldsymbol{r}_j - \boldsymbol{r}_i|\right) \tag{4}$$

for incompressible fluid, the particle number density remains constant.

2.2.3 Gradient model

The gradient model is used to discretize the pressure gradient in the governing equation. The expression is:

$$\langle \nabla P \rangle_i = \frac{D}{n^0} \sum_{j \ne i} \frac{P_j + P_i}{|\boldsymbol{r}_j - \boldsymbol{r}_i|^2} (\boldsymbol{r}_j - \boldsymbol{r}_i) W(|\boldsymbol{r}_j - \boldsymbol{r}_i|) \tag{5}$$

where D represents the dimension and represents the initial particle number density.

2.2.4 Divergence model

Similar to the gradient model, the divergence model is used to discretize the velocity divergence in the governing equation. The expression is:

$$\langle \nabla \cdot \boldsymbol{V} \rangle_i = \frac{D}{n^0} \sum_{j \neq i} \frac{(\boldsymbol{V}_j - \boldsymbol{V}_i) \cdot (\boldsymbol{r}_j - \boldsymbol{r}_i)}{|\boldsymbol{r}_j - \boldsymbol{r}_i|^2} W(|\boldsymbol{r}_j - \boldsymbol{r}_i|) \tag{6}$$

2.2.5 Laplacian model

Laplacian model is used to discretize the second derivative in the governing equation, which can be expressed as:

$$\langle \nabla^2 \phi \rangle_i = \frac{2D}{n^0 \lambda} \sum_{j \neq i} (\phi_j - \phi_i) W(|\boldsymbol{r}_j - \boldsymbol{r}_i|) \tag{7}$$

where λ represents the correction of the error introduced by the kernel function, and it can be written as:

$$\lambda = \frac{\sum_{j \neq i} W(|\boldsymbol{r}_j - \boldsymbol{r}_i|) |\boldsymbol{r}_j - \boldsymbol{r}_i|^2}{\sum_{j \neq i} W(|\boldsymbol{r}_j - \boldsymbol{r}_i|)} \tag{8}$$

2.3 Pressure Poisson equation

In the MPS method, the Poisson equation is used to solve the particle pressure. The incompressibility of fluid is determined by divergence-free condition and constant particle number density condition. The Poisson equation adopted in this paper is as follows:

$$\langle \nabla^2 P^{k+1} \rangle_i = (1-\gamma) \frac{\rho}{\Delta t} \nabla \cdot \boldsymbol{V}_i^* - \gamma \frac{\rho}{\Delta t^2} \frac{< n^k >_i - n^0}{n^0} \tag{9}$$

where superscripts k and k+1 represent k and k+1 time steps. is a variable parameter, representing the proportion of particle number density in the source term of Poisson equation. In the numerical simulation in this paper, takes 0.01. (Tanaka and Masunaga (2010), Lee et al. (2011))

2.4 Detection of free surface particles

When solving the Poisson's pressure equation, it is very important to determine whether a particle is located on a free surface. The number density of particles can be used to determine whether a particle is on a free surface in MPS method, as figure 1 shows. When $\langle n \rangle_i < 0.8 n^0$, the particle is considered to be on a free surface. When $\langle n \rangle_i > 0.97 n^0$, the particles are thought to be inside the fluid. For particles with particle number density between 0.8 and 0.97, it's difficult to tell whether the particle is on the free surface or inside the fluid. Khayyer and Gotoh (2010) first proposed the criterion which simply based on the fact that for a free-surface particle, the distribution of neighboring particles is asymmetric. In this paper, the vector function $\boldsymbol{F}$ presented by Zhang et al. (2012) is introduced, as follows:

$$< \boldsymbol{F} >_i = \frac{D}{n^0} \sum_{j \neq i} \frac{(\boldsymbol{r}_i - \boldsymbol{r}_j)}{|\boldsymbol{r}_i - \boldsymbol{r}_j|} W(|\boldsymbol{r}_i - \boldsymbol{r}_j|) \tag{10}$$

If $\langle |\boldsymbol{F}| \rangle_i > 0.9 |\boldsymbol{F}|^0$, the particle i will be considered to be on a free surface. $|\boldsymbol{F}|^0$ stands for $|\boldsymbol{F}|$ at the initial time of the free surface particle.

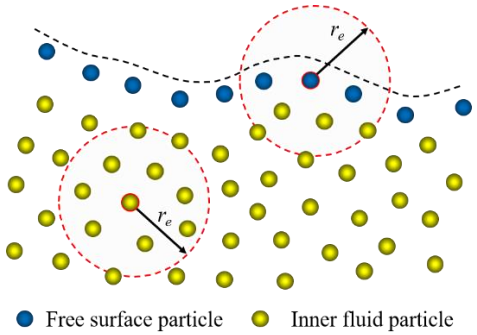

Figure1. Schematic diagram of free surface particle judgment.

3 NUMERICAL SIMULATION

In this section, the inner solver MPSGPU-SJTU is used to simulate the two-dimensional water inlet process of the damaged cabins. Firstly, the stability and accuracy of the method are verified by simulating the water inlet process of two-dimensional square cabin with side opening, and compare the motion of the cabin with the existing results.

3.1 Validation of the Method

As shown in Figure 1, the model is a square tank with a side length of 0.1m and an opening of 0.02m above the side. Other specific parameters are shown in Table 1. The water inlet process of this model is simulated. The calculation domain is 0.4m long and 0.3m wide, the initial particle spacing is 0.05mm, and the time step is 0.001s, with a total of 20000 time steps. The fluid density is 1000kg/m^3, the Kinematic viscosity coefficient equals to 1×10^{-6}m^2/s, and the total number of particles is 88613, including 72375 fluid particles and 3350 boundary particles.

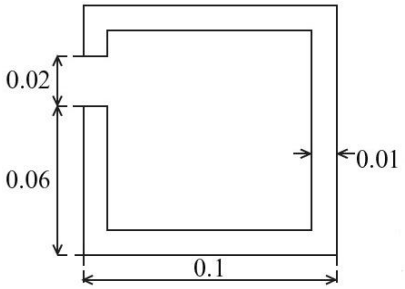

Figure 2. Schematic diagram of 2D cabin section

Table 1. Model scale parameters

parameter	value
wight/kg	7.5
moment of inertia/kg*m2	0.075
Length/m	0.1
Height/m	0.1
center of gravity height/m	0.025
Thickness/m	0.01
ship draft/m	0.075

The simulation results of MPS are compared with those obtained by VOF and SPH method, as shown in Figure 2. The figure shows the fluid field and the hull motion. From top to bottom are the results of VOF, SPH and MPS methods, and from left to right are 0.1s, 0.2s, 0.3s and 0.4s respectively. It can be seen from the figure that the results obtained by these three methods are in good agreement. At 0.1s, the fluid begins to enter the cabin. The fluid reaches the bottom of the shelter at 0.2s. At 0.3s, the fluid accumulates on the right side of the bottom and impacts the right bulkhead. At 0.4s, the fluid starts to accumulate on both sides, and the fluid on the right is more than that on the left. The results of MPS simulation are in good agreement with the existing results, whether the cabin motion pattern or the fluid distribution in the cabin.

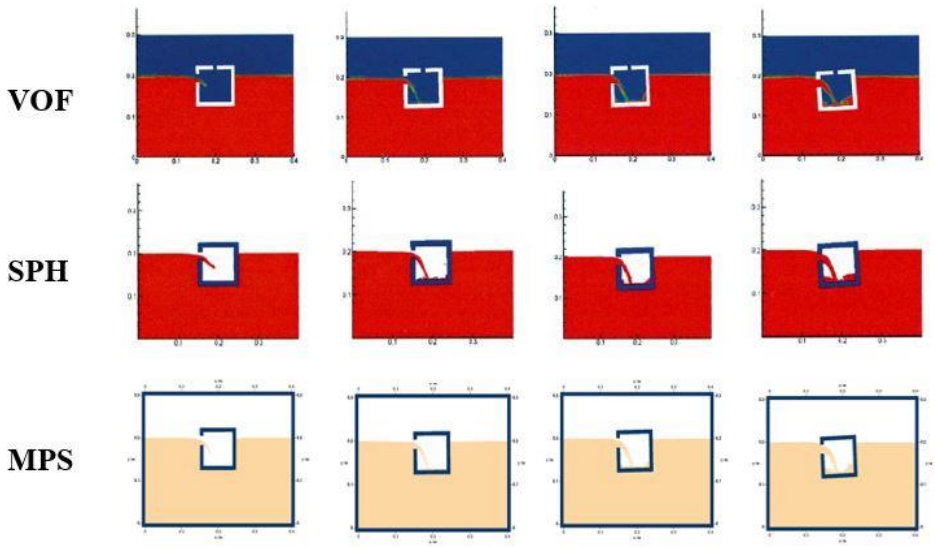

Figure 3. Comparison of the calculated results with the existing one.(From left to right: 0.1s, 0.2s, 0.3s, 0.4s. From top to bottom: VOF, SPH, MPS.)

Figure 4 shows the horizontal and vertical acceleration comparison between MPS method and SPH method. It can be seen that the heave acceleration has a relatively large oscillation at the beginning, and the vibration amplitude turns to small and agrees well with the SPH method. The sway acceleration oscillates around 0, and the amplitude is much smaller than that in the vertical direction. It is in good agreement with the SPH method, too. The above analysis fully shows that the MPSGPU-SJTU solver can well simulate the flooding process of a damaged hull.

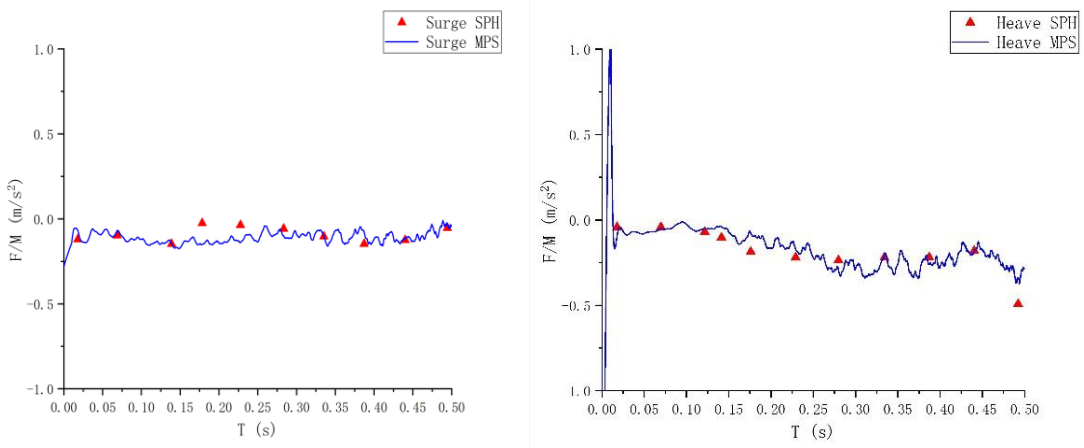

(a) (b)

Figure 4. (a) Horizontal and (b) vertical acceleration comparison

3.2 Water inlet simulation of the broken tank with a horizontal baffle

In this section, the water taking in process of a broken cabin with horizontal baffle is simulated by MPS method. The same horizontal baffle is arranged at the side walls of the cabin at different heights, as figure 5 shows.

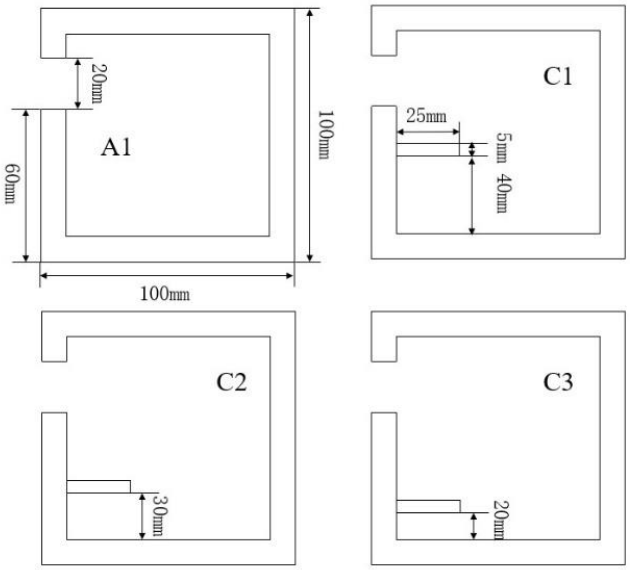

Figure 5. Schematic diagram of 2D cabin section with a horizontal baffle.

The initial position of the broken cabin is the same as in Section 3.1. The cabin is released from stillness and falls freely. The horizontal and vertical displacement, and the roll angle are recorded and the time histroy curve is drawn in figure 6.

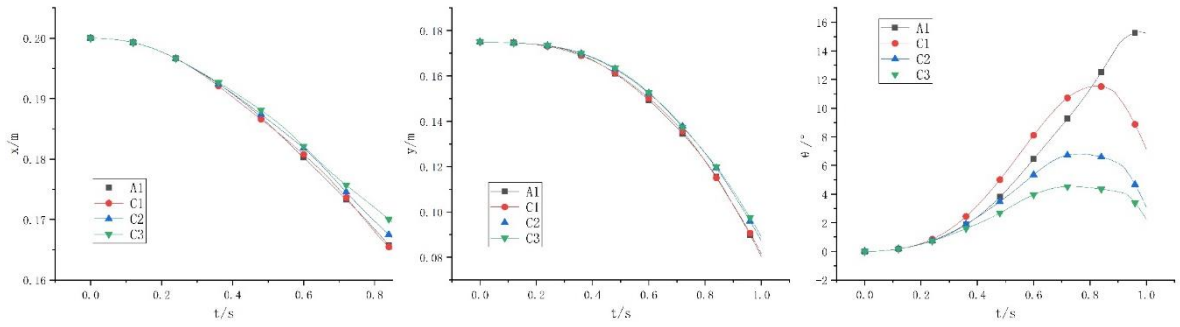

(a) (b) (c)

Figure 6. Time history curve of (a) Horizontal and (b) vertical displacement and (c) roll angle.

It can be seen from Figure 6 (a) that the position of the horizontal baffle has little influence on the horizontal displacement of the cabin. The horizontal displacements of the C1 model are similar to that of A1, and the horizontal displacements of the other two horizontal models with lower baffle positions, C2 and C3, are smaller. The horizontal displacements of these models differ by no more than 7% at most. It can be obtained that the horizontal baffles arranged in the cabin will reduce the horizontal displacement, and the horizontal baffles with lower position are better.

It can be seen from Figure 6 (b) that the horizontal baffles arranged in different positions in the cabin also have little influence on the vertical displacement. The vertical displacement of the C1 model with higher horizontal baffle position is similar to that of A1, and the other two horizontal models with lower horizontal baffle position C2 and C3 both have smaller vertical displacement of A1. The vertical displacements of these models differ by no more than 5%. It can be obtained that the horizontal baffles arranged in the cabin will affect the vertical displacement, and the horizontal baffles in the lower position will reduce the vertical displacement and rate, which can effectively extend the submergence time, thereby increasing the escape and rescue time.

It can be seen from Figure 6 (c) that, the horizontal baffles arranged at different positions have a great influence on the roll of the broken cabin. Due to the horizontal baffle, the maximum roll angle becomes smaller, and the time to reach the maximum roll angle is also shorter, which is very different from the above conclusions of horizontal and vertical displacement. The lower the position of the horizontal baffle, the smaller the maximum roll angle is. And the time to reach the maximum roll angle is shorter. The maximum roll angle of A1, C1, C2 and C3 is 15 °, 12 °, 7 ° and 5 °. The time to reach the maximum roll angle of is 0.98s, 0.82s, 0.73s and 0.72s, respectively. So it can be concluded that the reasonable arrangement of the horizontal baffle in the cabin can reduce the roll angle of the ship, thereby win more rescue time.

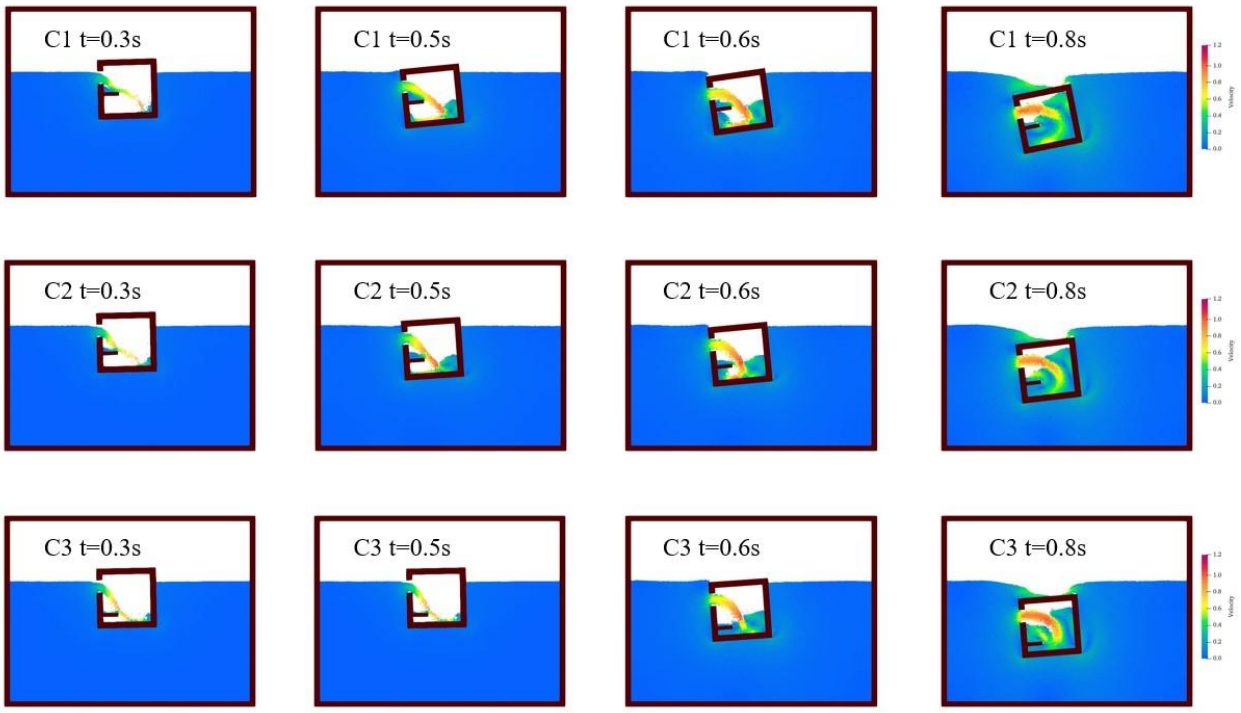

Figure 7. Velocity distribution in the process of breaking into water

Figure 6 shows the velocity distribution of the water intake process of the broken cabin with a horizontal baffle. It can be seen that the velocity of the water is small at the initial time. Fluid accumulates on the horizontal baffle, and the amount of accumulated fluid is C1>C2>C3, so that the roll angle of C1 is significantly larger than that of C3.

3.3 Water inlet simulation of the broken tank with a vertical baffle

In this section, the water intake process of a broken cabin with vertical baffle is simulated. The same vertical baffle is arranged at the bottom of the cabin at different positions, as figure 8 shows. The horizontal and vertical displacement, and the roll angle are recorded and the time history curve is drawn in figure 6.

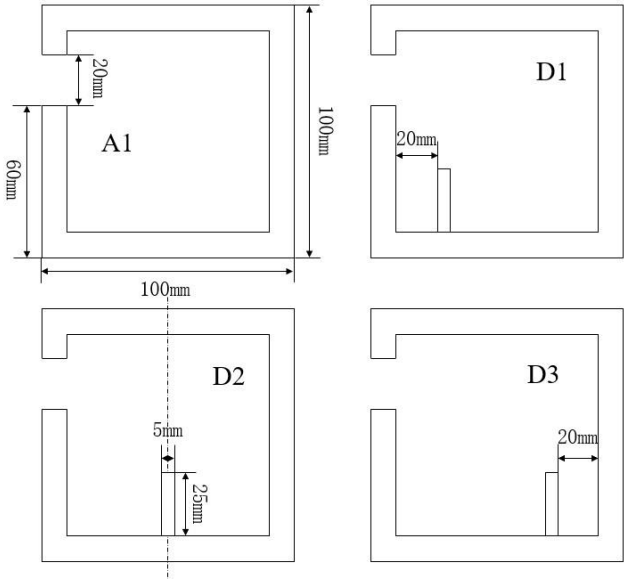

Figure 8. Schematic diagram of 2D cabin section with a vertical baffle.

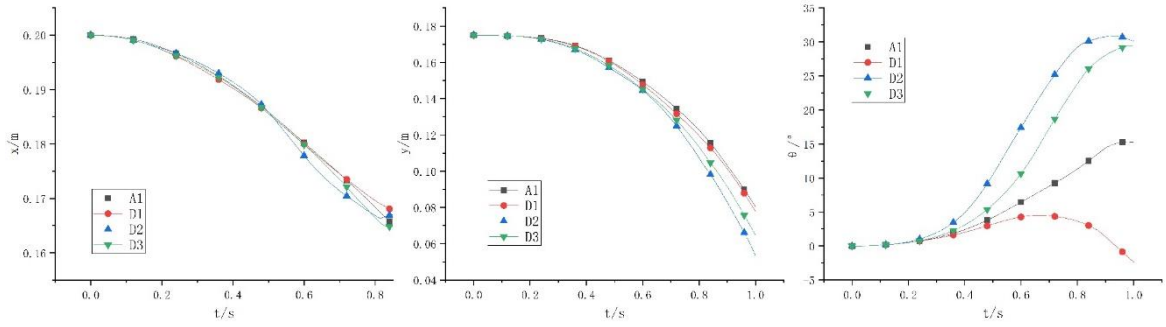

(a) (b) (c)

Figure 9. Time history curve of (a) Horizontal and (b) vertical displacement and (c) roll angle.

It can be seen from figure 9(a) that the position of the vertical baffle has little influence on the horizontal displacement of the broken cabin. Moreover, the horizontal displacements of D1 and D2 are smaller than those of the baffle-free model A1. It can be seen from figure 9 (b) that the position of the vertical baffle will affect the vertical displacement. The vertical displacement and rate of C1 are similar to those of A1 without vertical baffles, and the vertical displacement of the other two cases C2 and C3 are larger, and the difference of the vertical displacement can reach 26% at most. It can be seen from Figure 9 (c) that the position of the vertical baffle has a great influence on the rolling motion of the broken cabin when the water taking in. The closer the vertical baffle is to the opening, the smaller the maximum roll angle is. At the same time, the time for D1 to reach the maximum roll angle is much faster than other models.

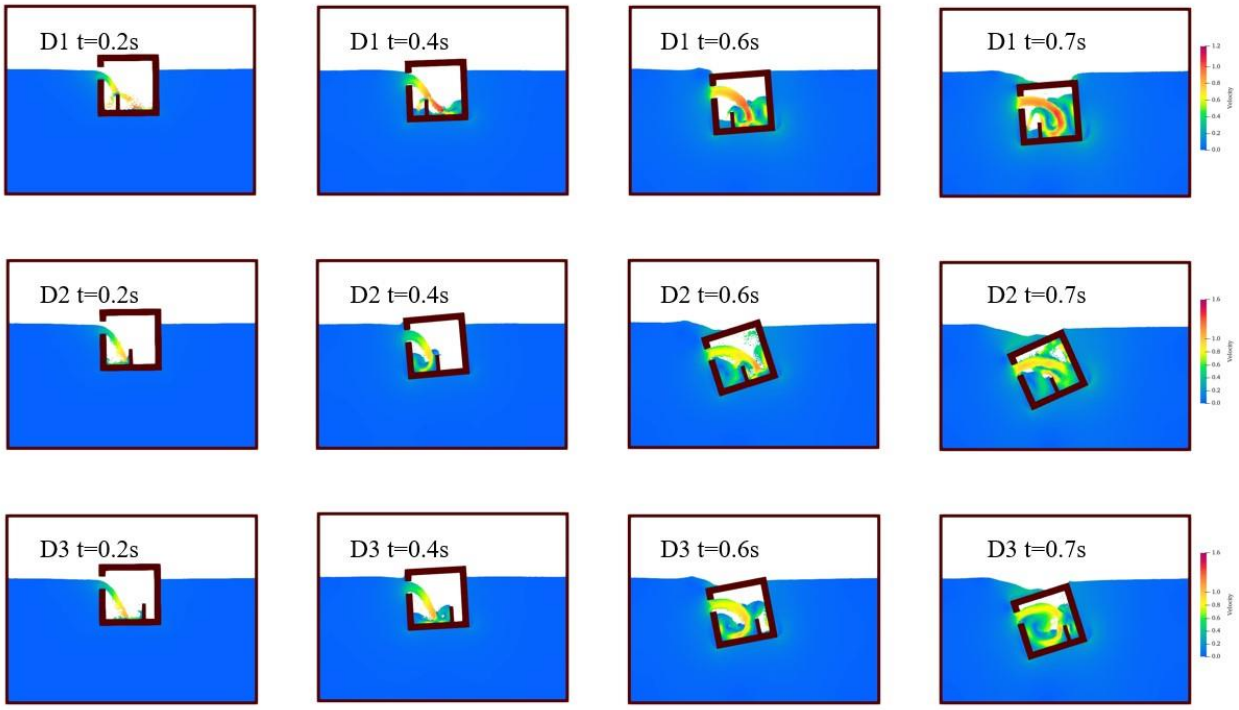

Figure 10. Velocity distribution in the process of water intake of the broken cabin.

Figure 10 shows the velocity distribution of the water intake process of the broken cabin with a vertical baffle. It can be seen from the figure 10 that the fluid is diverted from the beginning by the vertical baffle. In D1 case, the vertical baffle separates the fluid to the left and right, and D2 and D3 make the fluid gather on the left side. At t=0.6s, the fluid in D1 and D2 directly reaches the right side from the opening due to the roll of the cabin, while in D3 case, the fluid still all accumulates on the left side. Thus, it can be concluded that deploying the baffles in the appropriate position can make the fluid distribution in the cabin uniform and reduce the roll angle.

4. CONCLUSIONS

In this paper, the water intake process of a broken cabin with horizontal and vertical baffle is simulated by the in-house solver MPSGPU-SJTU. For the cases with horizontal baffle, the position of the horizontal baffle has a small impact on horizontal and vertical displacement, but a significant impact on the roll angle. The baffle changes the trajectory and distribution of fluid. The results show that the horizontal baffle at a lower position has a better effect on reducing roll angle and extending rescue time. For the cases with vertical baffle, the position of the baffle has little impact on horizontal and vertical displacement, but a great impact on the roll angle. The results show that arranging vertical baffles in appropriate positions can divert the fluid, distribute the fluid evenly on both sides, reduce roll angle, and extend rescue time. On the contrary, if the vertical baffle is placed in an inappropriate position, it will exacerbate the fluid distribution asymmetry and accelerate the capsizing of the cabin.

ACKNOWLEDGEMENTS

This work was supported by the National Natural Science Foundation of China (52131102), and the National Key Research and Development Program of China (2019YFB1704200), to which the authors are most grateful.

REFERENCES

Cao, X. Y., Ming, F. R., Zhang, A. M., Tao, L. (2018). Multi-phase SPH Modelling of Air Effect on the Dynamic Flooding of a Damaged Cabin. *Computers & Fluids*, 163: 7-19.

González, V., Talens, M., Riola, J. M., Valle, J., & Espin, M. (2003). Numerical prediction of the dynamic behavior of a Ro-Ro ship after a hull side damage. *Proceedings of the 8th International Conference on Stability of Ships and Ocean Vehicles*, Madrid, 215-227.

Khayyer, A., Gotoh, H. and Shao, S. (2010). Enhanced predictions of wave impact pressure by improved incompressible SPH methods. *Applied Ocean Research*, 31(2), 111-131.

Lee, B. H., Park, J. C., Kim, M. H., Hwang, S. C. (2011). Step-by-step improvement of MPS method in simulating violent free-surface motions and impact-loads. *Computer Methods in Applied Mechanics and Engineering*, 200, 1113-1125.

Ming, F. R., Zhang, A. M., Cheng, H., Sun, P. N. (2018). Numerical simulation of a damaged ship cabin flooding in transversal waves with smoothed particle hydrodynamics method. *Ocean Engineering*, 165: 336-352.

Shen, L.， Vassalos, D. (2009). Applications of3D parallel SPH for sloshing and flooding. *Proceedings of the 10th International Conference on Stability of Ships and Ocean vehicles*, St. Petersburg, 723-732.

Tanaka, M. and Masunaga, T. (2010). Stabilization and Smoothing of Pressure in MPS Method by Quasi-Compressibility. *Journal of Computational Physics*, 229(11), 4279–90.

Touzé, D. L., Marsh, A., Oger, G., Guilcher, P. M., & Ferrant, P. (2010). SPH simulation of green water and ship flooding scenarios. *Journal of Hydrodynamics*, 22(5), 231-236.

Zhang, A. M.， Cao, X. Y.， Ming, F. R.， Zhang, Z. F. (2013). Investigation on a damaged ship model sinking into water based on three dimensional SPH method. *Applied ocean research*, 42, 24-31.

Zhang, G. Y., Wu, J. X., Sun, Z., Moctar, O., Zong, Z. (2020). Numerically simulated flooding of a freely-floating two-dimensional damaged ship section using an improved MPS method. *Applied Ocean Research*, 101, 102207.

Zhang Y., Wan, D. (2012) Apply MPS method to simulate liquid sloshing in LNG tank. *Proc. of the 22nd Int. Offshore and Polar Eng. Conf.* (Rhodes, Greece) 381-91.

Zhang, Y., Wan, D., Hino, T. (2014a). Application of MPS method in liquid sloshing. *The China Ocean Engineering*, 32(4), 24-32.

Zhang, Y., Wan, D., Hino, T. (2014b). Comparative study of MPS method and level-set method for sloshing flows. *Journal of Hydrodynamics*, 26(4), 577-585.